

Fast, In-Situ Repair of Aircraft Panel Components

S. Dehm* and D. Wurzel†

German Aerospace Research Establishment (DFVLR), Stuttgart, Federal Republic of Germany

In this paper, three fields of activity on the fast repair of aircraft composite panels are presented. These activities involved studies to repair delaminations in thin panels by resin injection. The delaminations were caused by impacting the panels in a drop weight tower. The injection method seems feasible; however, both panel sides must be accessible. Secondly, a glass/epoxy leading-edge component was repaired by different approaches. The component then was tested under bending and torsion. The photoelasticity method was found to be a valuable instrument to study the efficiency of the applied repair procedures and thus to further develop a qualified repair technique. Finally, flat CFRP panels and stringer-stiffened panels with simulated damages were repaired and tested. Special emphasis was placed on employing repair techniques that would enable the fast and simple but substantial restoration of strength and stiffness of the damaged section on the spot, under limited accessibility. Testing the panels under compression and torsion loads gave promising results.

Introduction

COMPOSITE materials are playing an ever increasing role in military and civil aircraft. Their application in both secondary and primary structures has created a need for adequate repair procedures. The DFVLR Institute for Structures and Design is investigating repair techniques that will enable short-term repairs of aircraft composite components. The aim of the investigations is the restoration of the aerodynamic efficiency as well as the strength and stiffness required for full-flight spectrum capability, if for a limited time only. To avoid the effort and time needed for dismantling the damaged structures, the repair must be possible on the spot or after the complete structure is removed from the aircraft. Therefore, only those repair techniques are considered which allow work under limited accessibility to the damaged structure and without sophisticated equipment.

The institute's repair investigations centered on repair techniques for composite panels predominantly for fighter aircraft. The work concentrated on three main fields of activity: 1) repair of panel delaminations by resin injection, 2) repair of through-the-thickness damages in panels, including stiffened panels, and 3) suitability of the photoelasticity method to judge repair quality. The results obtained so far are presented in detail in this paper.

Repair of Delaminations by Resin Injection

Depending on their size, delaminations may cause the degradation of properties in laminates. Therefore, large-size delaminations need to be repaired. In the present study, composite panels 150 × 150 mm in size were impacted in a drop weight facility. The panel material was Celion 6K/Code 69 graphite/epoxy. The layup was

$$(0_2 / \pm 45 / 90 / \pm 45 / 0_2)_s$$

leading to a total of 18 layers. The impact conditions were chosen such that a maximum delamination size without obvious additional damages was achieved. Using a blunt 30-mm-diam impactor dropped from 0.8 m resulted in delaminations of about 60 mm in diameter. The delamination size was determined by ultrasonic C-scan, and its outline was

marked on the panel. In the approximate center of the delamination area, a blind hole leaving the last two layers (0.2 mm) intact was drilled as an injection hole. The diameter was 3.5 mm. At the periphery, blind holes 1 mm in diameter were drilled to serve as suction holes. Optimum diameters and hole arrangements were determined in a series of tests. With the existing conditions, four suction holes proved to be sufficient.

The epoxy resin system selected was Rütapox CY 160 N/SL due to its low viscosity (Fig. 1) and excellent wetting capability. The injection setup is explained in Fig. 2. To repair the delaminations, both the resin and the damaged area were heated. The resin was pressed into the injection hole. The resin flow into the delaminations was improved when the laminate was heated slightly higher than the resin. Spreading of the resin was supported by applying vacuum to the suction holes. When the resin emerged from the suction holes, the injection procedure was stopped. To cure the resin, the panels were

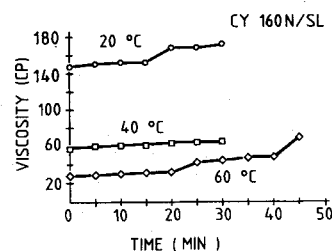


Fig. 1 Viscosity vs time of Rütapox CY 160 N/SL for different starting temperatures.

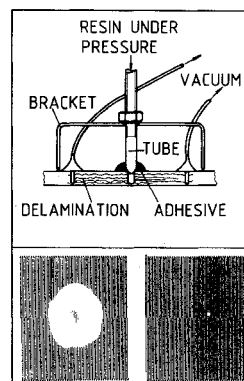


Fig. 2 Resin injection into delaminated plates (top), C-scans before and after resin injection (bottom).

Received Nov. 12, 1986; presented as Paper 86-4.6.2 at the 15th Congress of the International Council of Aeronautical Sciences (ICAS), London, England, Sept. 7-12, 1987; revision received Sept. 11, 1987. Copyright © 1986 by ICAS and AIAA. All rights reserved.

*Dipl.-Ing., Institute for Structures and Design.

†Dr.-Ing., Institute for Structures and Design.

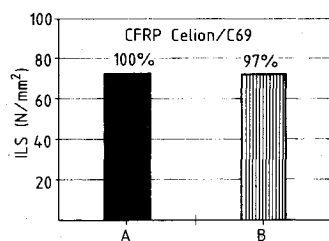


Fig. 3 Interlaminar shear strength of CFRP panels (a) and repaired impact damaged panels after resin injection (b).

heated and kept at 80°C for 2 h, and mechanical pressure was also added. The panels were postcured at RT for 12 h. (Curing at RT only would require 24 h.) To determine the degree of resin penetration, the panels then were u-scanned again, and ILS tests were also performed. The best results were obtained with panel and resin temperatures of 60 and 40°C, respectively. Under these conditions, the delaminated areas could be almost totally filled with resin (Fig. 2), and the interlaminar shear strength of the repaired section was restored to nearly the original strength (Fig. 3). Coupons cut from damaged areas would mostly separate into two pieces of different thickness, indicating a major delamination plane.

However, one severe problem was encountered with some of the impacted test panels. Here the impact had also caused cracks in the bottom of the panel opposite the impact area through which the resin could escape during the injection phase. These cracks could not be detected with the ultrasonic C-scan method. The resin flow through any cracks could be stopped if access to the rear side were available. Thus, although a restoration to full strength seems possible, the resin injection method is not ideally suited for on-the-spot repairs, because both sides need be accessible, which is in contradiction to the demand to be applicable under limited accessibility.

Photoelastic Inspection

To help improve repair techniques and to judge the efficiency of the repair, reliable testing methods are needed. X-ray radiographic and ultrasonic inspection are accepted NDT methods detecting delaminations, flaws, voids, and other imperfections; however, they do not convey any information on the performance, e.g., of adhesive joints and load introductions or load paths. While this information can be gained by strain gage measurements, these are limited to discrete points. Therefore, attention was centered on the photoelastic method, which allows extensive observation of complete areas. The component surface is covered with a photoelastic layer. The component wall thickness should be small in order to let the surface strains be representative of the component strains. When the component is loaded and viewed under a reflection polariscope, colored lines give evidence of strain distributions. Isochromatic lines represent constant values in the difference of the principal strains. While no absolute strain values can be obtained without additional measurements, the photoelastic method yields qualitative information on the load distribution in the component. Therefore, it should be well suited as a tool in the development of qualified repair techniques.

To get positive evidence of this assumption and to check the effort needed to get meaningful results, a series of tests was run. These tests involved simple tensile test coupons, leading-edge components, and panels. The test samples had circular or elliptical cutouts to simulate damages, some of which had been repaired by different methods. The photoelastic measurements were supported by strain gage measurements to obtain quantitative results. The leading-edge components, loaded under bending and torsion, had been selected as representative "real" aircraft structures to find out whether the photoelasticity method is also helpful when both the shape

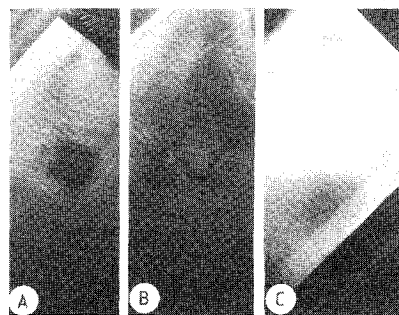


Fig. 4 Evaluation of different repair steps by the photoelasticity method.

of the component and the stress/strain distributions are more complex. The materials used in these tests were graphite/epoxy for the tensile and panel coupons and glass/epoxy for the leading-edge components.

From these tests it was found that the photoelasticity method allows one to compare different repair methods and assess their performance. An example is given in Fig. 4 which shows circular cutouts in a leading-edge component. A circular patch was bonded to the bottom surface of the leading-edge skin. The patch had been slit over half the diameter so it could be introduced through the cutout from the top surface. Then the hole in the skin was closed with a cotton fiber/resin mixture or by laminating in place a glass/epoxy insert. In both cases the cutout edges remain clearly visible due to limited load flow into the inserts. The cotton/resin filler cannot restore an adequate load flow over the slit as can the glass/epoxy filler (Figs. 4a and 4b). Figure 4c shows a scarfed elliptical patch with a good load flow.

Practical experience and care, however, are required to distinguish repair-induced disturbances in the strain behavior from irregular strain patterns. The patterns result from uneven load distributions in the structure due to complicated shapes and laminate construction. Also, much care must be used during the application of the photoelastic layer. Geometric parameters like sharp curvatures or narrow radii may distort the results, as may creep and environmental effects. These are some of the features that limit the practical use of the photoelasticity method for monitoring the quality of repairs of aircraft structures. But in the laboratory, the photoelasticity method is a very valuable tool in the development of repair techniques.

Repair of Through-the-Thickness Damages

Some damages in panels and substructures make necessary the removal of the impaired sections. This entails replacement with fresh material or installation of patches to close the cutouts. The aim is to avoid damage propagation and restore lost qualities. The investigation presented in this paper aims at repairing damaged composite materials under the following provisions:

- 1) The repair must be possible with access to the damaged structural component from one side only.
- 2) The repair material is a composite material identical or related in composition to the parent laminate.
- 3) No sophisticated equipment is necessary.
- 4) The aerodynamic contour is to be vastly restored.

Based on these demands and taking into account available literature and also some previous though unpublished work of our own, the scarfed patch technique was selected in two versions: version 1 employed as patch material the same prepreg material that was used for the parent laminate, and version 2 employed a wet laminating technique. The components to be repaired were unstiffened or stringer-stiffened panels. Future work will include curved panels and panels with spar/rib subcomponents. To simulate limited accessibility, a metal frame was built onto which the panels can be fixed

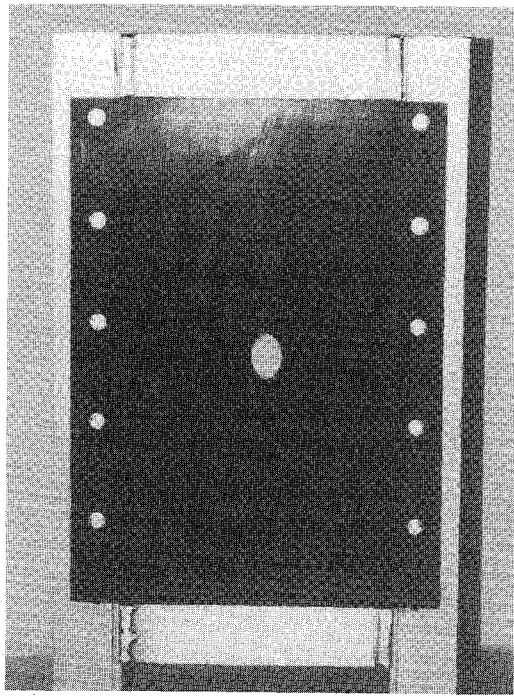


Fig. 5 Repair frame to simulate accessibility from the front only.

(Fig. 5). The panels can be positioned horizontally or vertically. While only flat panels were used so far, the frame can be modified to accommodate curved panels as well. Maximum panel size is 500×350 mm.

Material and Dimensions

The material selected was Narmco's Rigidite 5245C reinforced with IM400 fibers. This modern carbon fiber prepreg system is specifically designed for aerospace application and is available in the U.S. and Europe. The IM400 fiber was chosen for reasons of fast availability. For the same reason, the resin content of the prepreg was 39%. Uncured ply thickness was 0.16 mm, cured ply thickness 0.136 mm. The layup for both the unstiffened and stringer stiffened panels was

$$(0_2 / \pm 45 / 90 / \pm 45 / 0_2)_S$$

resulting in an anisotropic laminate of 18 layers. Total thickness was 2.45 mm. The characteristic construction of the stringer-stiffened panels followed a technique used by Dornier Co. for its design of a CFRP wing for the Alpha-Jet.¹ U-shaped sections were joined together on a base laminate, with the junction planes forming symmetry planes. The stiffened panels were manufactured in one shot in an autoclave. Aluminum bars covered with thermal expansion rubber were used for forming the u-sections and served as pressure pieces in the autoclave.

Also in accordance with the Alpha-Jet wing skin, the panel/stringer dimensions were

$$s_{\text{blade}} = s_{\text{blade}} \text{ and } 2h_{\text{blade}} = b_{\text{stringer}}$$

In the present investigation, the absolute values of the panel skin thickness (s_{skin}) and the stringer height (h_{blade}) were 2.45 mm and 20 mm, respectively. Influenced by the testing machine dimensions, the test panel size was 420×230 mm.

Damage Simulation and Repair

In order to get reproducible results, circular sections 51 mm in diameter were cut out of the panels in the center region. For the stringer-stiffened panels, this also meant the disruption of the central stringer. With a panel width of 230 mm, this resulted in a panel width-to-diameter ratio of 4.5. As for the

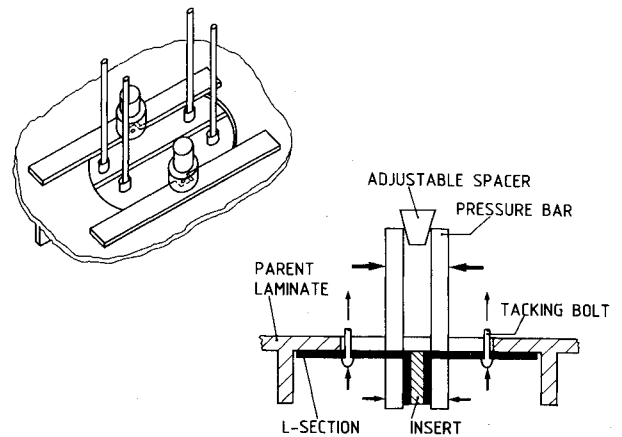


Fig. 6 Positioning and bending in place of stringer repair elements.

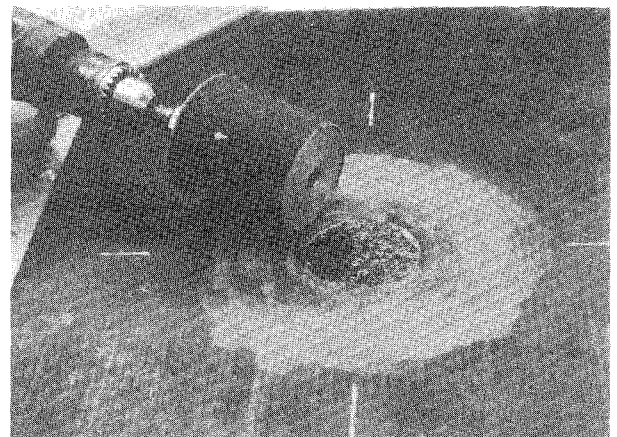


Fig. 7 Scarfing of cutout.

cross-sectional areas, the remaining area of the damaged yet unscarfed panel was 78% of the undamaged reference panel, both for the unstiffened and stringer-stiffened panels. This was considered to be more realistic than the frequently selected 60% in other studies. Both repair versions required a stiff base plate so the repair layers could be laminated in place. The base plate for the unstiffened panels consisted of two parts, each measuring 80×40 mm in size so they could be introduced through the opening in the panel. The plates were manufactured from two layers of carbon cloth and Ciba Geigy Ly556/Hy917/Dy062 epoxy resin. The two halves were glued to the bottom of the parent laminate with a quick-acting adhesive. Tacking bolts were used to position the plates and keep them in place during bonding. In the case of the stringer-stiffened panels, the stringers were repaired first by bonding in place two L-sections and replacing the missing stringer section with an insert (Fig. 6). The L-sections were 120 mm long, the legs measuring 20 and 38 mm, corresponding to the stringer height and the stringer spacing, respectively. The material used for the sections was IM400/5245C, the layup was

$$(0_2 / \pm 45 / 90 / \pm 45 / 0_2)_T$$

the adhesive was Scotch-Weld 7236 B/A, cured 30 min at 80°C . The repaired stringer (L-sections and insert) would also serve as a lamination support.

The next step was scarfing the cutout with a scarf ratio of 20:1 (Fig. 7). The outer scarf diameter was marked on the surface, and so were the fiber directions. The tool used was a handheld drilling machine with a conical grinding head. The sanding paper, grain size 80, was fixed with double-sided adhesive tape. Grinding the scarf needs some experience to get a clean surface. The outlines of the individual layers may serve

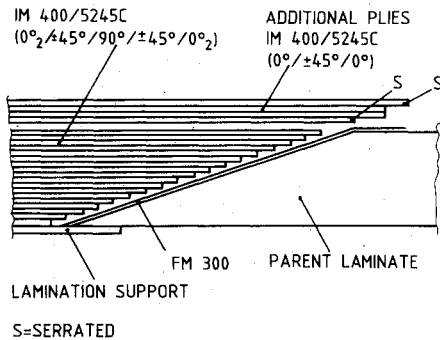


Fig. 8 Composition of prepreg patch.

as guidelines as they become visible. The lamination support kept the bottom plies from fraying during the grinding operation. If unsupported, unidirectional plies especially tend to fray. After the scarf was finished, the tacking bolt holes and any uneven spots in the lamination supports were removed by a putty coat of short carbon fibers and Scotch-Weld 7236 B/A.

The final step in the repair procedure was closing the cutout in the panel by laminating a patch in place. In version 1, the patch material was IM400/5245C and the layup was identical with the parent laminate, but with four additional layers on top to make up for the lower ILS strength of the patch (Fig. 8). The decrease in the ILS strength was a consequence of the missing autoclave pressure. To cure the patch, only heat and vacuum were applied. This led to an ILS value of 47.7 N/mm² compared to 79.5 N/mm² reached with identical but autoclave cured test coupons. The individual layers for the patch were water-jet cut with diameters increasing in 5- and 6-mm steps from 50 to 170 mm to match the scarf. The four overlapping top layers had orientations of 0 and ± 45 deg, and the 0-deg layers were serrated to improve load introduction by shear.² The patch was built up outside the cutout, starting with the top layer. Due to tackiness, the layup had to be done carefully, as no position changes were possible once a ply had been placed. An FM 300 film adhesive was put on the scarfed cutout, and then the patch was mounted in place. Vacuum was applied, and as no heat blanket was available, curing at 180°C was done in an oven for 2 h.

The material used for version 2 was Brochier G 808 carbon fiber cloth with a warp/weft ratio of 10:1 and Ly556/Hy988 epoxy resin. This resin system was selected because of its good thermal stability.³ To prevent a distortion of the cloth plies during resin impregnation, a release foil was coated with the resin. The cloth was placed on the resin side of the foil, and the individual layers were cut to size along previously marked outlines on the other side of the foil, again with stepwise increasing diameters. The scarfed cutout and the lamination support were also coated with resin. Then each ply was positioned in the cutout, the foil was removed, and the next ply was added. Due to the higher ply thickness of 0.3 mm, only 11 plies were needed. The layup was (0/+45/-45/0), plus three additional overlapping layers orientated in the 0- and ± 45 -deg directions. No layer with a warp direction of 90 deg was used due to the presence of the weft filaments of the 0 deg-dominated cloth layers. Again, curing took place in an oven at 160°C for 3 h. In addition to the vacuum, a weighted cover plate proved to be necessary to get an even surface of the wet laminated patch. The ILS strength was measured to be 37.4 N/mm.²

In an effort to inspect the repaired sections with NDT methods, two unstiffened panels, each repaired with one of the two repair versions, were subjected to x-ray radiographic inspection. No effort was made to use the C-scan method. Previous experiments with test samples had indicated unsatisfactory results when the C-scan method was used with the two repair versions described due to microporosity caused by the

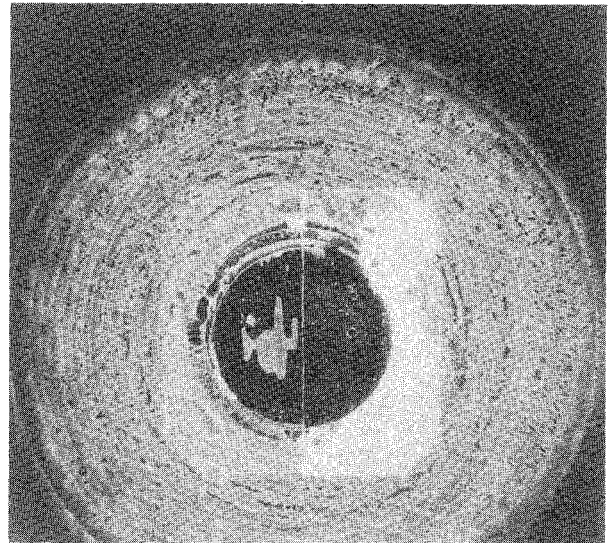


Fig. 9 X-ray inspection of a panel repaired with a prepreg patch—individual plies and lamination supports are clearly visible.

lack of curing pressure. The x-ray picture of the patch manufactured from prepreg material shows a marked difference between the parent laminate and the patch (Fig. 9). Besides many voids, the structure of the patch is clearly visible, predominantly between adhesive film and patch. This phenomenon is indicative of the missing pressure and was also observed with another prepreg system in our previous work. Also visible are the two halves of the lamination support plate. The dark areas were caused by an x-ray opaque penetrant, indicating that the bonding technique used here is sufficient to let the plates act as supports but would be inhibitive to any load-carrying function. Amazingly, the wet laminated patch was hardly discernible from the parent laminate; only the lamination supports were clearly visible. Considering the test results reported later on, it becomes obvious that the x-ray technique can tell little about the load-carrying capability of the repaired sections.

Experimental Setup and Tests

The experimental setup comprised a 400-kN universal testing machine for compression loading and a hydraulic torsion rig to introduce torsional loads. The torsion rig was suspended in front of the panel, and the four push/pull rods were connected to the load introductions (Fig. 10). The ends of the panels, stiffened and unstiffened, were inserted in metal "shoes" that served as load introduction. A firm rubber had been cast into the open spaces in the shoes, so that there was no direct lateral contact between the metal and the panel ends except for two spacers at each corner. Thus, compression loads were introduced directly into the panel end faces, while torsion loads were transferred via the rubber, which helped to limit end constraints. The spacers assisted in the torsional load introduction and kept the panel ends in their relative positions within the shoes.

Two sets of panels, with and without stringers, were tested. Each set comprised four panels:

- REF: undamaged reference panel
- DAM: panel with unscarfed cutout
- R-PRP: panel repaired with prepreg patch
- R-WET: panel repaired with wet laminated patch

Up to 43 strain gages—single gages and 0/45/90-rosettes—were bonded to different parts of each panel. A complete data accumulation cycle lasted less than 5 ms and was followed by a 2-s interval. Additionally, all repaired panels and the damaged stiffened panel were covered with a photoelastic layer.

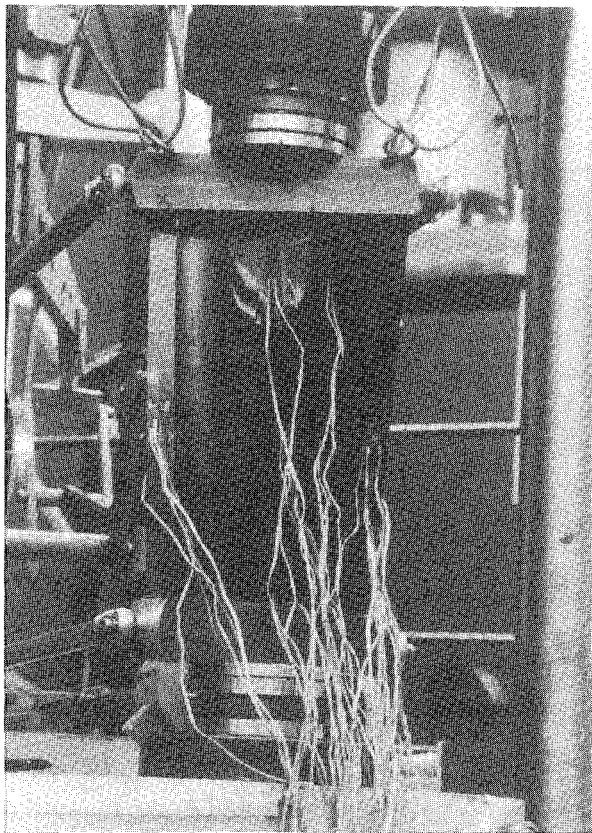


Fig. 10 Experimental setup for compression and torsion loading.

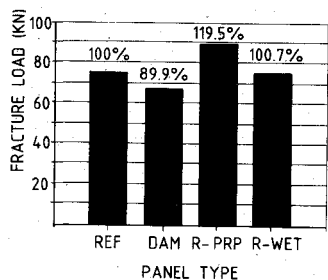


Fig. 11 Compression loads at failure.

The panels were subjected to torsion, compression, and combined torsion and compression. All tests so far were done at RT and ambient humidity. As no antibuckling devices were used in the tests up to now, the unstiffened panels would bend from the beginning under compression loading. The maximum torsional load of 58 Nm induced a 10-deg angle of twist between the panel ends. Load tests of the unstiffened panels are being continued. They mainly serve the purpose of getting more experience with the photoelastic method and observing the load flow between parent laminate and patch.

One set of stiffened panels was loaded to fracture: First, the maximum torsional load was applied, then compression was added till the panel failed. Loading time till fracture was about 60–80 s. The torsional load was 58 Nm; the additional compression load at failure is given in Fig. 11. Related to the cross-sectional area of the undamaged panel under pure compression, these loads would correspond to compression stresses between 83 and 100 N/mm². The combined loading and the buckling of the panels resulted in a complex deformation and stress distribution, however. The longitudinal strain distribution across the panel midsection may be taken to characterize the panel deformation.

Twisting of the ends and compression led to compressive strains at the panel edges on both the front and rear sides, while the panel center buckled out of plane, causing tensile

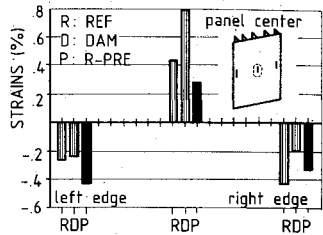


Fig. 12 Longitudinal strains before failure at the mid-section of the panel front side.

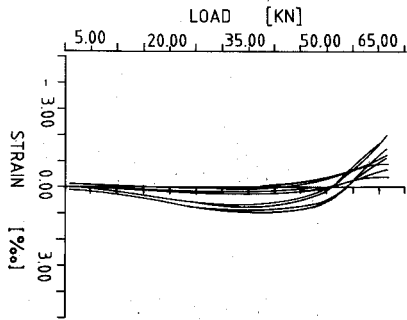


Fig. 13 Characteristic behavior of stringer strains.

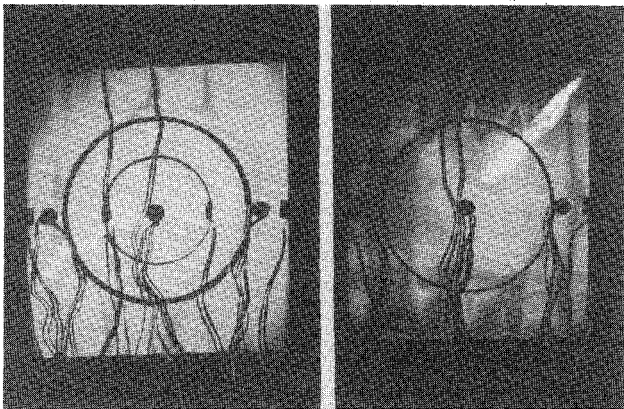


Fig. 14 Photoelastic pictures of repaired panels. Left: wet laminated patch; right: prepreg patch. Irregular strain behavior of wet laminated patch indicates early failure.

strains on the front side and compressive strains on the rear or stringer-stiffened side (Fig. 12). Another clear indication of the panel buckling, e.g., was the strain behavior of the stringers with a strain reversal from tensile to compressive strains (Fig. 13). The highest strains measured prior to failure and close to the edges of the cutout were 0.78%. Otherwise, maximum strains in the last complete measuring cycle did not exceed about 0.5%. Compared to the reference panel, the repaired panels were stiffer in the repaired section, as is evident from the reduced strains. From the strain behavior it can be taken that instability was the dominating factor for failure.

Concerning fracture, the undamaged REF panel and the P-PRP panel on one side and the DAM and R-WET panels on the other exhibited similar behavior. The REF and R-PRP panels were broken diagonally. On the R-PRP panel, the fracture zone stayed in the parent laminate and closely followed the outline of the patch. The patch did not debond. The R-PRP panel had carried substantially more load than the REF panel.

The DAM panel was broken horizontally in the center across the cutout and so was the R-WET panel, as fracture was initiated by the debonding of the patch. The R-WET panel failed on the same load level as the REF panel. If the adhesion between patch and parent laminate could be

improved, both repair techniques might be equally efficient. That the wet laminated patch was the weak spot in the R-WET panel test that would lead to failure was clearly made evident by the photoelastic method (Fig. 14). In contrast to the prepreg patch, the color patterns here indicated an uneven load introduction and high principal strain differences in the scarf area.

Conclusion and Outlook

The tests described in this paper were intended to use repair techniques on panels under limited access and to study their efficiency and their effect on the panel behavior under loading. Most repairs so far were tested to their strength. In this study tests were conducted in such a way that the stability of the panels would be the dominating criterion. Also, a relation between damage size and panel size was selected which was thought to more realistically represent the conditions found on real aircraft panels.

It was found that under stability-controlled conditions, the repair of panels, including stiffeners by removing the damaged section and patching the cutout, can successfully restore the original qualities. In the case of the prepreg patch, the failure loads were considerably higher than in the undamaged reference panel. Because of this wide margin, the number of overlapping layers will be reduced in the tests to follow. Although this will further reduce the patch strength, this seems permissible if stability is the reigning factor. This also improves the smoothness of the surface. In the case of the wet laminated patch, the repair was less successful, as the patch separated from the panel. The wet lamination technique will be pursued, however. As the material components can be stored under more favorable conditions, this technique is considered to save costs. In the work to follow, therefore, more attention will be directed on load introduction from the

parent laminate into the patch and on improving the adhesion between patch and parent laminate.

An important and instructive instrument to judge the quality of the repair was found in the photoelastic method. This method is thought to be especially helpful in the investigation of the load introduction into the patch. More tests will be made involving simple loading conditions to increase our experience with this technique. Although excellent for laboratory purposes, the photoelastic method is too complicated to use in practical repair work. Therefore, the search will continue for an easily usable and interpretable method of testing repair quality.

In an ongoing study, the presence of moisture in the parent laminate during the repair process and the influence of environmental effects are being investigated. This study involves the materials mentioned in this report and different adhesives in the search for moisture-insensitive systems.

Acknowledgment

The testing department of the institute has contributed much to this paper. Special thanks go to R. Aoki and H. Kraft, who have given valuable help with the photoelastic inspection method and the testing.

References

- ¹Rose, D., Henze, E., Wurzel, D., and Schelling, H., "Design of a CFRP Wing for the Alpha-Jet-Major Panel Tests," *Proceedings of the AIAA/ASCE/AHS 26th Structures, Structural Dynamics and Materials Conference*, Orlando, FL, April 15-17, 1985, Part 1, pp. 446-453.
- ²Kiger, R.W. and Beck, C.E., "Large Area Composite Repair," *Proceedings of the 33rd Annual Technical Conference*, Washington, DC, 1978, Section 17-D, pp. 1-8.
- ³Niederstadt, DFVLR-Braunschweig/FRG, personal communication.

*New from the AIAA
Progress in Astronautics and Aeronautics Series . . .*



Commercial Opportunities in Space

F. Shahrokhi, C. C. Chao, and K. E. Harwell, editors

The applications of space research touch every facet of life—and the benefits from the commercial use of space dazzle the imagination! *Commercial Opportunities in Space* concentrates on present-day research and scientific developments in "generic" materials processing, effective commercialization of remote sensing, real-time satellite mapping, macromolecular crystallography, space processing of engineering materials, crystal growth techniques, molecular beam epitaxy developments, and space robotics. Experts from universities, government agencies, and industries worldwide have contributed papers on the technology available and the potential for international cooperation in the commercialization of space.

TO ORDER: Write AIAA Order Department,
370 L'Enfant Promenade, S.W., Washington, DC 20024
Please include postage and handling fee of \$4.50 with all orders. California and D.C. residents must add 6% sales tax. All orders under \$50.00 must be prepaid. All foreign orders must be prepaid.

1988 540pp., illus. Hardback
ISBN 0-930403-39-8
AIAA Members \$49.95
Nonmembers \$79.95
Order Number V-110